Supplementary Information

Polymerization-pH Tailored RAFT-Mediated Polymerization-Induced Self-assembly for Ice Recrystallization Inhibiting Investigation

Huangbing Xu,[a,b] *Teng Qiu,*[a,b,c] *Haotian Shi,*[a] *Xiaoqian Tian,*[b] *Xiaoyu Li,*[*,a,b] *Longhai Guo*[*,a.b,c]

a. State Key Laboratory of Organic-Inorganic Composites, Beijing University of Chemical Technology, Beijing 100029, PR China.

b. Key Laboratory of Carbon Fiber and Functional Polymers, Ministry of Education, Beijing University of Chemical Technology, Beijing 100029, PR China.

c. Beijing Engineering Research Center of Synthesis and Application of Waterborne Polymer, Beijing University of Chemical Technology, Beijing 100029, PR China

Corresponding Authors

*E-mail for Longhai Guo: guolh@mail.buct.edu.cn;

*E-mail for Xiaoyu Li: lixy@mail.buct.edu.cn

Table of Content

1. Synthesis of ***S,S'***-bis (***R,R'***-dimethyl-***R'***-acetic acid)-trithiocarbonate (BDAAT)

Carbon disulfide (30.4 g, 0.4 mol), chloroform (119.4 g, 1.0 mol), acetone (58.1 g, 1.0 mol), and tetrabutylammonium hydrogen sulfate (2.68 g, 0.008 mol) were mixed with 133 mL n-hexane into a 2 L glass flask cooled with the ice-water mixture. 50 *wt*% Sodium hydroxide aqueous solution (224 g, 28 mol) was added dropwise into the flask over 90 min, the temperature was kept below 10 °C. Then 1000 mL water and 133 mL HCl were added to dissolve and acidify the mixture after 12 h reaction. The mixture was stirred for another 30 min with a nitrogen purge to remove excess acetone and filtered to get a yellow solid. The yellow solid was washed with water several times and dried in a vacuum oven. After that, further purification by recrystallization in acetone was carried out and the yellow crystalline solid was finally obtained. The benzyl-capped BDAAT was synthesized according to the reference.[1]

2. The [1]H-NMR and the Conversion

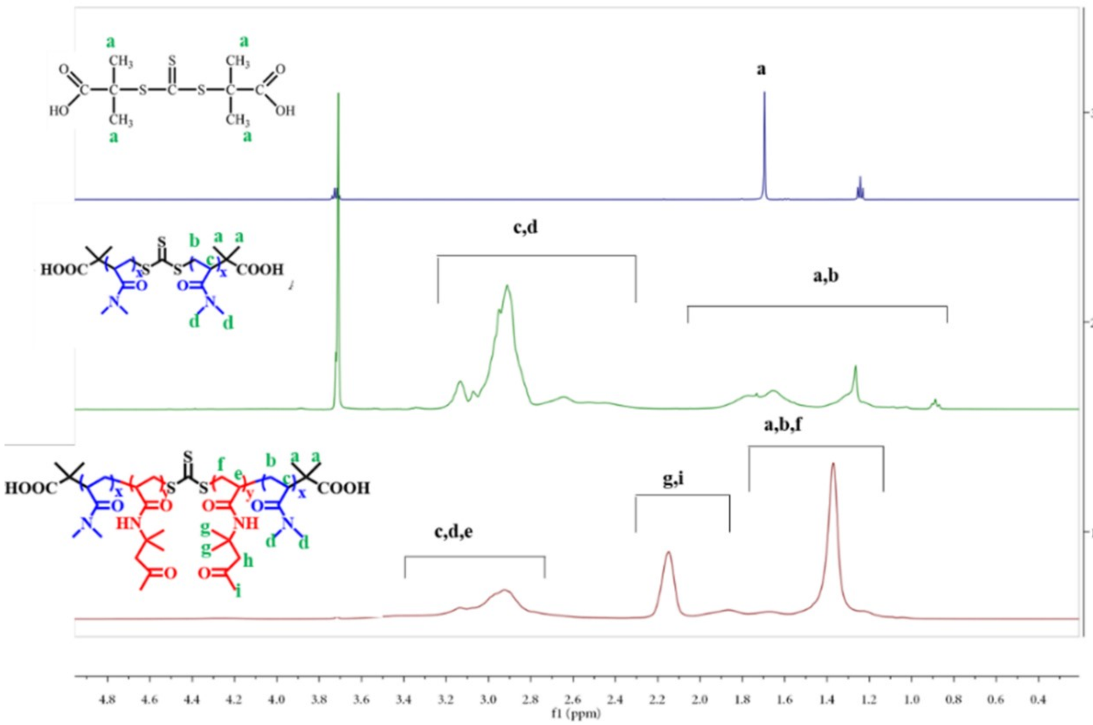

Figure S1. ^{1}H NMR spectra for BDAAT, PDMAA macro-CTA agent and PDMAA-*b*-PDAAM-*b*-PDMAA copolymer.

$$\text{conv}_{DMAA} = 1 - \frac{I_{6.75} + I_{6.08} + I_{5.64}}{3 \times DP_{th}} \times 100\% \tag{1}$$

$$\text{conv}_{DMAA} = 1 - 3 \times \left(\frac{I_{6.21} + I_{6.02} + I_{5.51}}{I_{2.16}} \right) \times 100\% \tag{2}$$

3. The FTIR Spectra

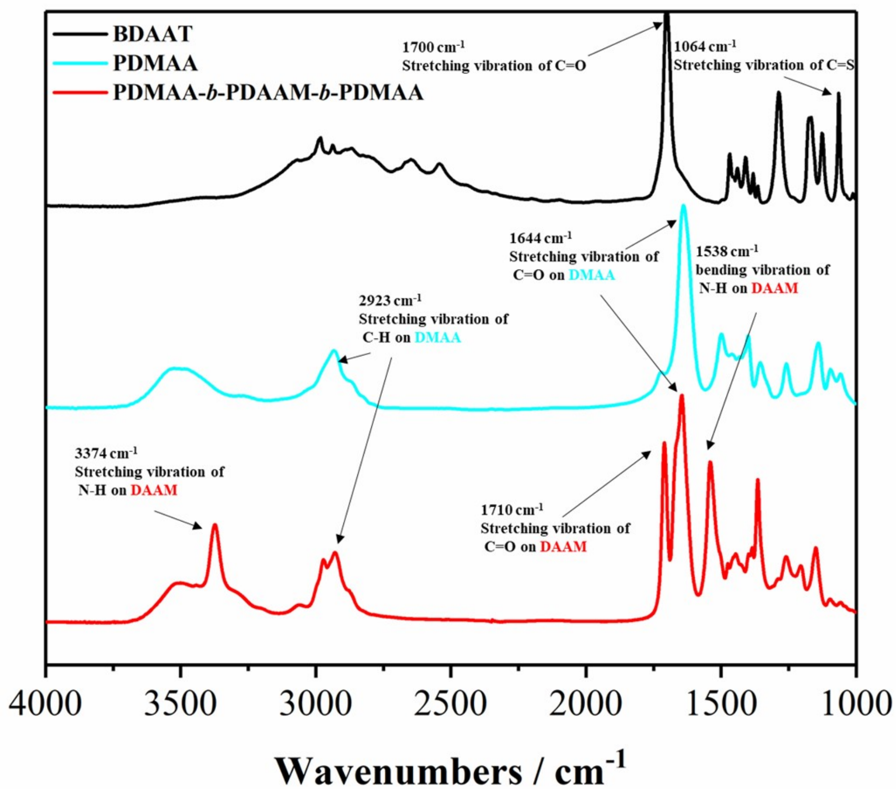

Figure S2. FTIR spectra of BDAAT, PDMAA macro-CTA agent and PDMAA-*b*-PDAAM-*b*-PDMAA triblock copolymer.

4. The Characterization Results of PDMAA Macro-CTAs

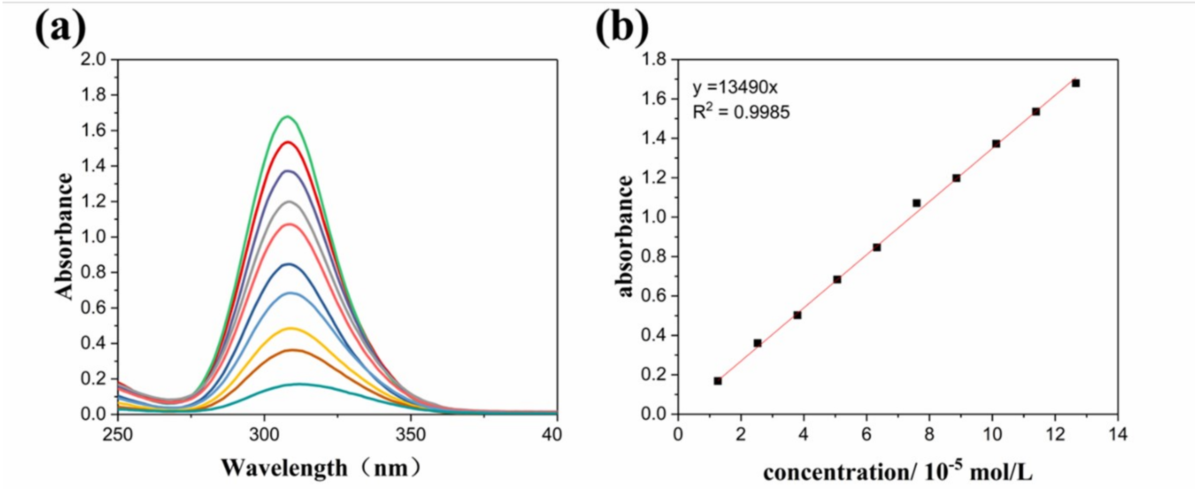

Figure S3. (a) UV spectra of BDAAT with different concentrations (1.26×10^{-5} mol/L ~ 12.6×10^{-5} mol/L) (b) and the calibration curve for concentration calculation.

by UV-vis using the peak at 308 nm for calibration. The calibration curve is provided in The mean DP for each macro-CTA was then determined in a methanol solution by the following equation:

$$DP = \frac{\frac{c_p}{c_{BDAAT}} - M_{BDAAT}}{M_m} \qquad (3)$$

where c_p stands for the concentration of PDMAA in methanol solution, c_{BDAAT} stands for the concentration of the BDAAT in methanol solution, and M_{BDAAT} and M_m stand for the molecular weight of BDAAT and monomer DMAA, respectively.

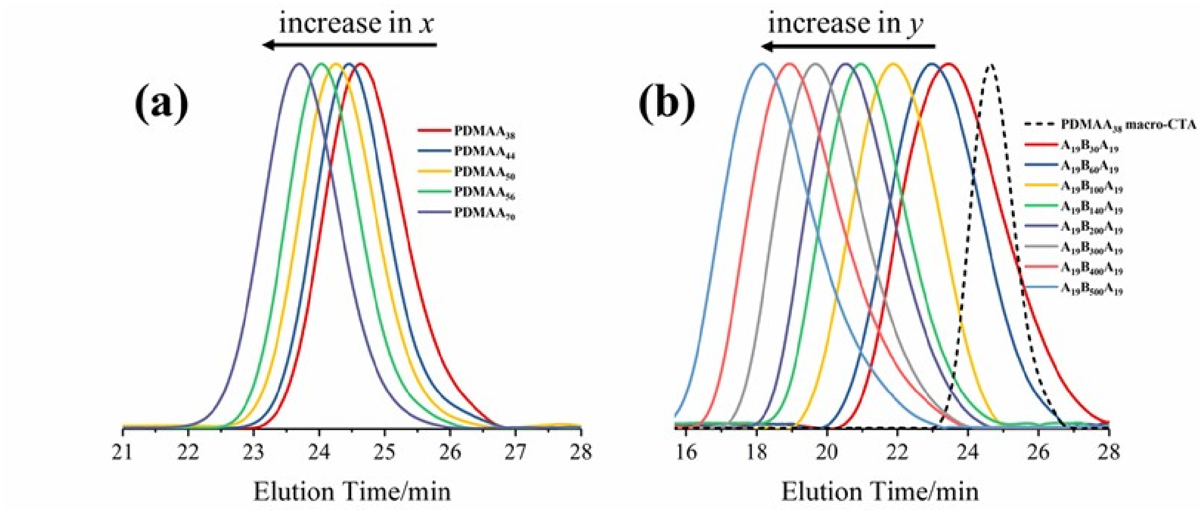

Figure S4. (a) Elution profiles of GPC for the characterization of $PDMAA_{2x}$ (x = 18, 22, 25, 28, 35); (b) Elution profiles of GPC for the characterization of $PDMAA_{19}$-*b*-$PDAAM_y$-*b*-$PDMAA_{19}$ (y = 30, 60, 100, 140, 200, 300, 400, 500)

Table S1. The characterization results of PDMAA macro-CTA with various DPs

Entry	Molecular Structure	Target DP	Conv.[a] %	Exp. DP[b]	x[c]	$M_{n,theo}$[d] / 10^3	$M_{n,\,GPC}$[e] / 10^3	M_w/M_n
1	$PDMAA_{38}$	30	> 99	38	19	3.3	3.8	1.14
2	$PDMAA_{44}$	40	> 99	44	22	4.2	5.1	1.12
3	$PDMAA_{50}$	50	> 99	50	25	5.2	5.4	1.18
4	$PDMAA_{56}$	55	> 99	56	28	5.7	6.4	1.12
5	$PDMAA_{70}$	60	> 99	70	35	6.2	8.9	1.19

[a] Monomer conversion calculated by ^{1}H NMR spectra

[b] Experimental DP calculated by UV spectra.

[c] x represents each block length of the asymmetrical $PDMAA_x$-*b*-CTA-*b*- $PDMAA_x$. x = DP/2.

[d] Theoretical M_n calculated by monomer conversion.

[e] M_n measured by GPC.

5. The Characterization Results of PDMAA$_x$-b-PDAAM$_y$-b-PDMAA$_x$ Triblock

Table S2. Summary of the characterization data for all PDMAA$_x$-PDAAM$_y$-PDMAA$_x$ triblock copolymers

Entry	2*x*	2*y*	pH	Conv. [a] /%	Z-average diameter/nm	PDI	$M_{n, Theo}$ [b] / 10^3 g·mol^{-1}	$M_{n, GPC}$ [c] / 10^3 g·mol^{-1}	Mw/ Mn	assigned morphology [d]
1	38	30	2.5	-	-	-	8.8	-	-	gel [e]
2		60		-	-	-	10.1	-	-	gel
3		100		-	-	-	16.9	-	-	gel
4		140		-	-	-	23.7	-	-	gel
5		200		-	-	-	33.8	-	-	gel
6		300		-	-	-	50.7	-	-	gel
7		400		-	-	-	67.6	-	-	gel
8		500		-	-	-	84.5	-	-	gel
9	38	30	6	-	-	-	8.8	-	-	gel
10		60		-	-	-	10.1	-	-	gel
11		100		-	-	-	16.9	-	-	gel
12		140		-	-	-	23.7	-	-	gel
13		200		-	-	-	33.8	-	-	gel
14		300		-	-	-	50.7	-	-	gel
15		400		-	-	-	67.6	-	-	gel
16		500		-	-	-	84.5	-	-	gel
17	38	30	8	100%	25	0.437	8.8	7.2	1.12	spheres
18		60		100%	37	0.259	10.1	10	1.30	spheres
19		100		100%	42	0.195	16.9	12.6	1.28	spheres+vesicles
20		140		100%	144	0.243	23.7	15.6	1.26	spheres+vesicles
21		200		100%	239	0.125	33.8	19.7	1.30	spheres+vesicles
22		300		100%	278	0.102	50.7	35.2	1.36	spheres+vesicles
23		400		100%	334	0.152	67.6	51.6	1.14	spheres
24		500		100%	338	0.071	84.5	66.8	1.42	spheres
25	44	40	2.5	-	-	-	11.1	-	-	gel
26		60		-	-	-	10.1	-	-	gel
27		80		-	-	-	13.5	-	-	gel
28		100		-	-	-	16.9	-	-	gel
29		120		-	-	-	20.3	-	-	gel
30		140		-	-	-	23.7	-	-	gel
31		160		-	-	-	27.0	-	-	gel

32		180		-	-	-	30.4	-	-	gel
33		200		-	-	-	33.8	-	-	gel
34		250		-	-	-	42.3	-	-	gel
35		300		-	-	-	50.7	-	-	gel
36		400		-	-	-	67.6	-	-	gel
37	44	40	6	-	-	-	11.1	-	-	gel
38		60		-	-	-	10.1	-	-	gel
39		80		-	-	-	13.5	-	-	gel
40		100		-	-	-	16.9	-	-	gel
41		120		-	-	-	20.3	-	-	gel
42		140		-	-	-	23.7	-	-	gel
43		160		-	-	-	27.0	-	-	gel
44		180		-	-	-	30.4	-	-	gel
45		200		-	-	-	33.8	-	-	gel
46		250		-	-	-	42.3	-	-	gel
47		300		-	-	-	50.7	-	-	gel
48		400		-	-	-	67.6	-	-	gel
49	44	40	8	97%	37	0.298	11.1	9.8	1.24	spheres
50		60		99%	56	0.147	10.1	10.7	1.32	spheres
51		80		95%	46	0.152	13.5	11.5	1.27	spheres
52		100		93%	65	0.08	16.9	14.3	1.35	spheres+vesicles
53		120		99%	86	0.073	20.3	15.1	1.4	spheres+vesicles
54		140		100%	107	0.05	23.7	16.2	1.25	spheres+vesicles
55		160		100%	152	0.069	27.0	18.8	1.19	spheres+vesicles
56		180		99%	175	0.115	30.4	19.3	1.34	spheres+vesicles
57		200		97%	186	0.064	33.8	20	1.32	spheres+vesicles
58		250		99%	192	0.057	42.3	28.3	1.35	spheres
59		300		96%	227	0.026	50.7	37.2	1.42	spheres
60		400		94%	254	0.102	67.6	59.8	1.36	spheres
61	50	60	2.5	-	-	-	15.1	-	-	gel
62		80		-	-	-	13.5	-	-	gel
63		100		-	-	-	16.9	-	-	gel
64		140		-	-	-	23.7	-	-	gel
65		160		-	-	-	27.0	-	-	gel
66		180		-	-	-	30.4	-	-	gel
67		200		-	-	-	33.8	-	-	gel
68		250		-	-	-	42.3	-	-	gel
69		300		-	-	-	50.7	-	-	gel
70		400		-	-	-	67.6	-	-	gel

71		500		-	-	-	84.5	-	-	gel
72	50	60	6	-	-	-	15.1	-	-	gel
73		80		-	-	-	13.5	-	-	gel
74		100		-	-	-	16.9	-	-	gel
75		140		-	-	-	23.7	-	-	gel
76		160		-	-	-	27.0	-	-	gel
77		180		-	-	-	30.4	-	-	gel
78		200		-	-	-	33.8	-	-	gel
79		250		-	-	-	42.3	-	-	gel
80		300		-	-	-	50.7	-	-	gel
81		400		-	-	-	67.6	-	-	gel
82		500		-	-	-	84.5	-	-	gel
83	50	60	8	96%	36	0.152	15.1	12.2	1.17	spheres
84		80		97%	63	0.092	13.5	13.7	1.19	spheres
85		100		98%	78	0.046	16.9	14.6	1.23	spheres
86		140		100%	168	0.117	23.7	16.8	1.28	spheres
87		160		99%	181	0.075	27.0	19.4	1.31	spheres
88		180		99%	184	0.053	30.4	19.7	1.22	spheres
89		200		100%	220	0.004	33.8	20.4	1.32	spheres
90		250		100%	193	0.045	42.3	30.6	1.33	spheres
91		300		99%	221	0.086	50.7	36.5	1.35	spheres
92		400		100%	259	0.044	67.6	60.7	1.43	spheres
93		500		99%	277	0.079	84.5	64.9	1.44	spheres
94	56	60	2.5	98%	33	0.146	15.7	11.2	1.20	spheres
95		80		99%	38	0.059	13.5	13.2	1.18	spheres
96		100		98%	56	0.019	16.9	14.9	1.39	spheres
97		120		99%	120	0.111	20.3	15.7	1.35	peanuts
98		140		100%	182	0.193	23.7	17.3	1.29	peanuts+worms
99		160		96%	316	0.358	27.0	19.5	1.37	peanuts+worms+vesicles
100		200		98%	607	0.222	33.8	24.2	1.25	tadpoles
101		250		99%	1398	0.245	42.3	33.7	1.38	tadpoles
102		300		99%	1139	0.217	50.7	40.0	1.25	tadpoles
103		350		98%	1718	0.262	59.2	55.6	1.40	tadpoles
104		400		97%	1237	0.191	67.6	61.7	1.40	vesicle string
105		450		99%	1692	0.235	76.1	67.5	1.38	vesicle string
106		500		100%	1955	0.292	84.5	71.1	1.42	vesicle string
107		550		100%	567	0.394	93.0	82.2	1.47	LCVs
108		600		100%	619	0.194	101.4	88.5	1.50	LCVs
109		700		100%	822	0.377	118.3	103.7	1.58	LCVs

110		800		100%	1025	0.142	135.2	115.4	1.57	LCVs
111	56	60	6	95%	46	0.151	15.7	11.1	1.26	spheres
112		80		98%	67	0.051	13.5	13.2	1.22	spheres
113		100		99%	101	0.049	16.9	14.6	1.37	spheres
114		120		97%	169	0.09	20.3	16.3	1.23	spheres
115		140		99%	198	0.091	23.7	17.7	1.38	spheres
116		160		100%	242	0.159	27.0	18.5	1.23	spheres+vesicles
117		200		96%	299	0.194	33.8	23.2	1.20	spheres+vesicles
118		250		98%	448	0.185	42.3	32.6	1.25	spheres+vesicles
119		300		99%	570	0.22	50.7	40.6	1.35	spheres+worms+vesicles
120		350		98%	1045	0.246	59.2	49.1	1.26	spheres+worms+vesicles
121		400		97%	837	0.569	67.6	54.9	1.34	spheres+vesicles
122		450		100%	525	0.141	76.1	59.0	1.40	LCVs
123		500		100%	619	0.24	84.5	69.3	1.39	LCVs
124		550		99%	638	0.118	93.0	72.0	1.46	LCVs
125		600		100%	663	0.287	101.4	81.3	1.54	LCVs
126		700		100%	690	0.31	118.3	101.7	1.55	LCVs
127		800		100%	756	0.277	135.2	114.6	1.57	LCVs
128	56	60	8	99%	39	0.242	15.7	12.3	1.29	spheres
129		80		99%	56	0.104	13.5	14.3	1.22	spheres
130		100		98%	74	0.089	16.9	14.9	1.29	spheres
131		120		100%	97	0.033	20.3	15.2	1.25	spheres
132		140		98%	115	0.024	23.7	16.8	1.37	spheres
133		160		100%	126	0.028	27.0	18.3	1.23	spheres
134		180		100%	164	0.066	30.4	23.9	1.33	spheres
135		200		100%	144	0.058	33.8	25.7	1.27	spheres
136		250		100%	177	0.05	42.3	30.4	1.38	spheres
137		300		100%	183	0.048	50.7	42.5	1.37	spheres
138		400		100%	202	0.042	67.6	46.4	1.34	spheres
139		500		99%	218	0.102	84.5	73.2	1.49	spheres
140		600		100%	234	0.107	101.4	80.5	1.54	spheres
141		700		100%	240	0.077	118.3	104.5	1.47	spheres
142		800		100%	245	0.17	135.2	117.6	1.51	spheres
143	70	100	2.5	100%	92	0.058	23.8	14.6	1.24	spheres
144		250		100%	155	0.241	42.3	34.6	1.21	spheres
145		400		100%	116	0.231	67.6	48.9	1.33	spheres
146		500		100%	105	0.226	84.5	72.4	1.24	spheres
147	70	100	6	99%	58	0.121	23.8	15.3	1.38	spheres
148		250		100%	118	0.027	42.3	35.5	1.38	spheres

149		400		100%	178	0.034	67.6	46.3	1.26	spheres
150		500		100%	170	0.064	84.5	73.6	1.40	spheres
151	70	100	8	98%	73	0.097	23.8	14.4	1.35	spheres
152		250		97%	113	0.033	42.3	32.7	1.37	spheres
153		400		100%	188	0.045	67.6	49.0	1.31	spheres
154		500		100%	208	0.046	84.5	75.8	1.31	spheres

a Determined by ^{1}H NMR spectroscopy;

b determined by DLS on 0.5 wt% dispersions diluted by 0.05M NaCl aqueous solution;

c $M_{n,theo} = DP_{PDMAA} \cdot M_{DMAA} + DP_{PDAAM} \cdot M_{DAAM}$;

d determined by TEM on 0.5 wt% dispersions diluted by 0.05M NaCl aqueous solution;

e gelation occurred as DP_{PDMAA} = 38, 44, 50 when the polymerization was performed under the pH= 2.5 or 6 at the midway of the PISA. All the PISA were conducted using a magnetic stirring at the bottom, gelation would occur from the top to the bottom of the dispersion and finally to a free-standing physical soft gel as the polymerization processed, which would lead to inaccuracy of the conversion and GPC and the morphology so the results were not recorded in this table.

6. Characterizations of $A_{28}B_yA_{28}$ Triblock Copolymers

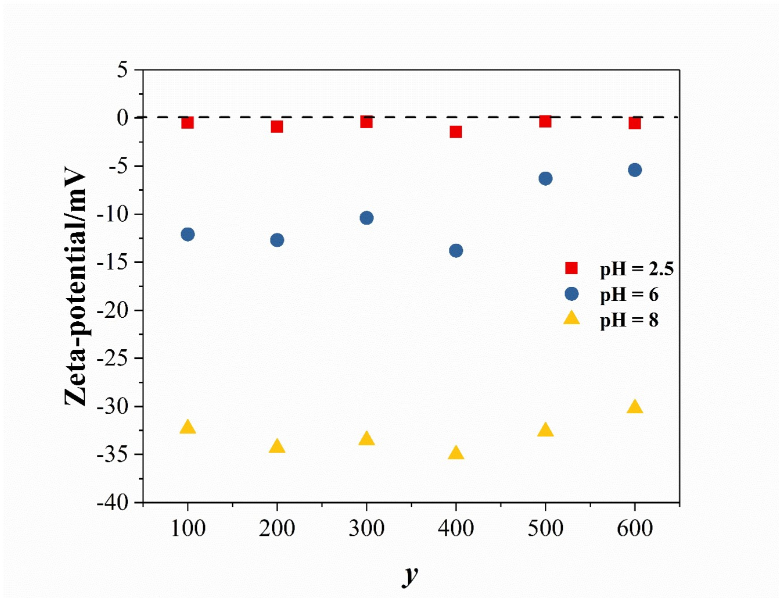

Figure S5. Zeta-potential for $A_{28}B_yA_{28}$ PISA particles prepared at different polymerization pH.

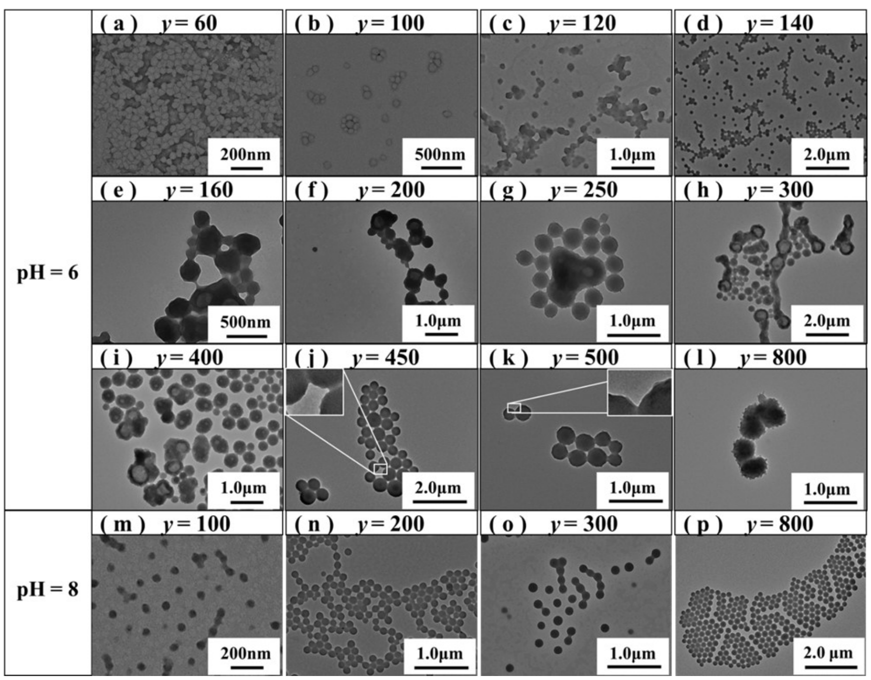

Figure S6. TEM images for $A_{28}B_yA_{28}$ PISA particles prepared at the polymerization pH = 6 (a-l), and 8 (m-p).

7. The Estimation of the Packing Parameter (*P*)

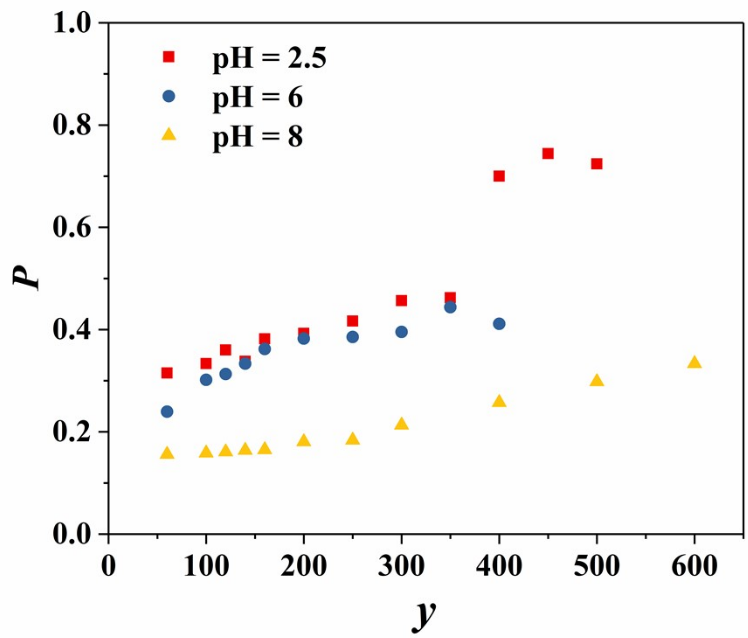

Figure S7. The evolution of packing parameter (*P*) as the function of *y* for PISA particles of $A_{28}B_yA_{28}$ prepared at different polymerization pH.

The basic data was from the TEM images. The packing parameter (*P*) is defined as :

$$P = \frac{v}{a_0 l_0} \tag{5}$$

where *v* is the volume of the hydrophobic segment, l_0 is the length of the hydrophobic segment, and a_0 is the effective area of the hydrophilic headgroups.[2]

The volume of the hydrophobic block *v* could be estimated through:

$$v = v_{DAAM}y \tag{6}$$

where v_{DAAM} is the volume of the DAAM monomer and y is the polymerization degree of the DAAM block.

l_0 is estimated by the radius (half of the average diameter, D) of the spheres and cylinders or the wall thickness of the vesicles. Therefore, the packing parameter could be calculated through:

$$P = \frac{2v_{DAAM}y}{a_0 D} \tag{7}$$

Assuming 1/3 as the critic value of P. At that point, spherical assemblies would be obtained. However, the morphology transition would happen as soon as the value of P exceeds 1/3. For example, for polymerization pH = 2.5, the $A_{28}B_{100}A_{28}$ could be chosen through the TEM images as at a transition critical point (P = 1/3), and a_0 can be calculated according to equation (7) by

$$\frac{1}{3} = \frac{2 * v_{DAAM} * 100}{a_0 * 63} \tag{8}$$

which gives $a_0 = 9.53v_{DAAM}$. Then the packing parameter of $A_{28}B_yA_{28}$ PISA particles under polymerization pH = 2.5 can be calculated. The packing parameters of $A_{28}B_yA_{28}$ nanoparticles under polymerization pH = 6 and 8 are calculated through the same method using $A_{28}B_{140}A_{28}$ and $A_{28}B_{600}A_{28}$ as the critical point, respectively. The diameter (D) of the particles (diameter of spheres and cylinders or the wall thickness of the vesicles) was the statistical results by the average of the diameters of ten particles in the TEM images for each sample via the software *Image J*.

8. The Kinetic Studies of $A_{28}B_{400}A_{28}$ Copolymers

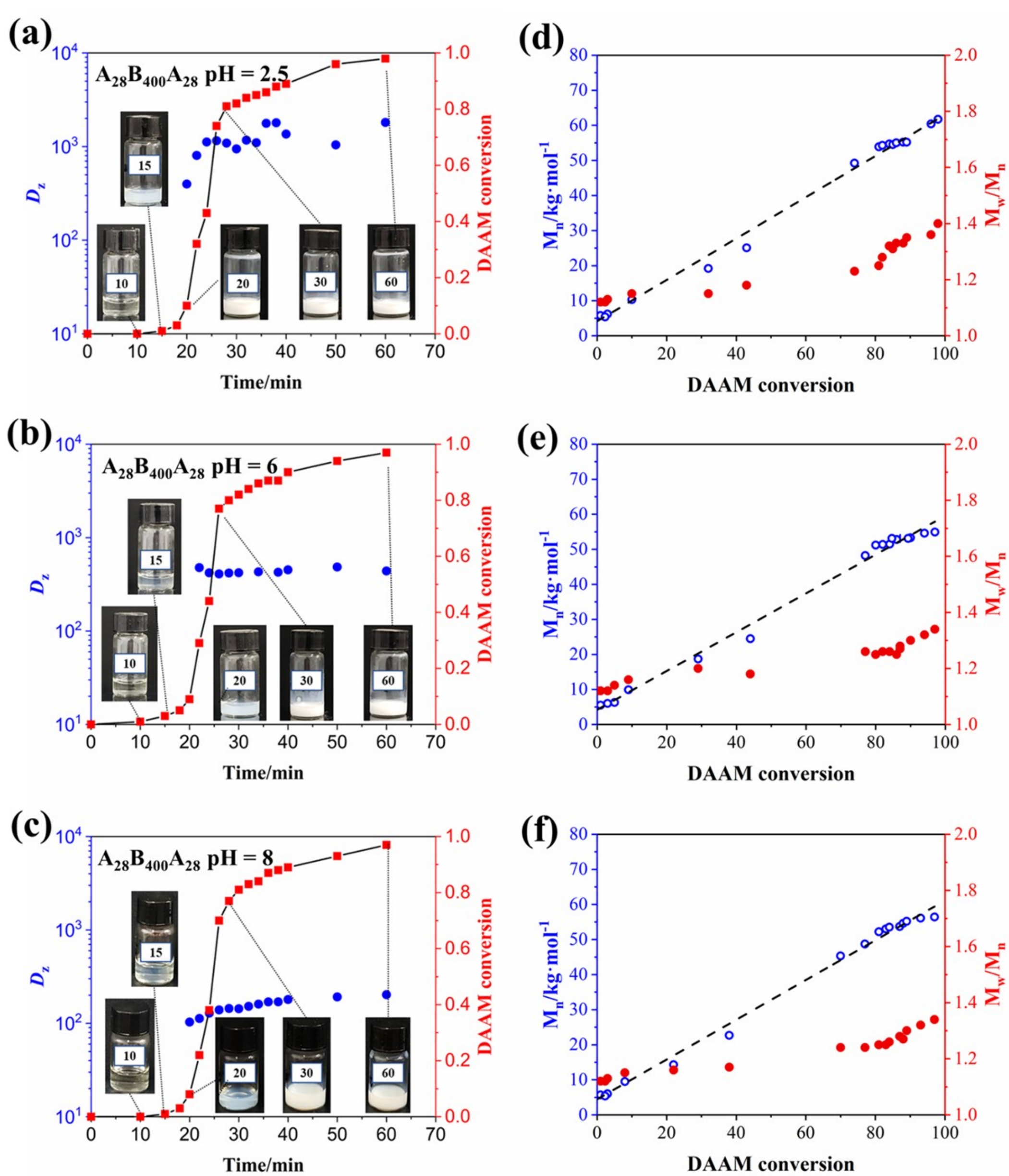

Figure S8. Plots of D_z (blue dots) and DAAM monomer conversion (red squares) as the function of time for $A_{28}B_{400}A_{28}$ polymerized at pH = (a) 2.5, (b) 6, (c) 8; evolution of M_n (blue circles) and dispersity (M_w/M_n, red dots) *vs*. DAAM conversion for the RAFT-PISA of $A_{28}B_{400}A_{28}$ polymerized at pH = (d) 2.5, (e) 6, (f) 8.

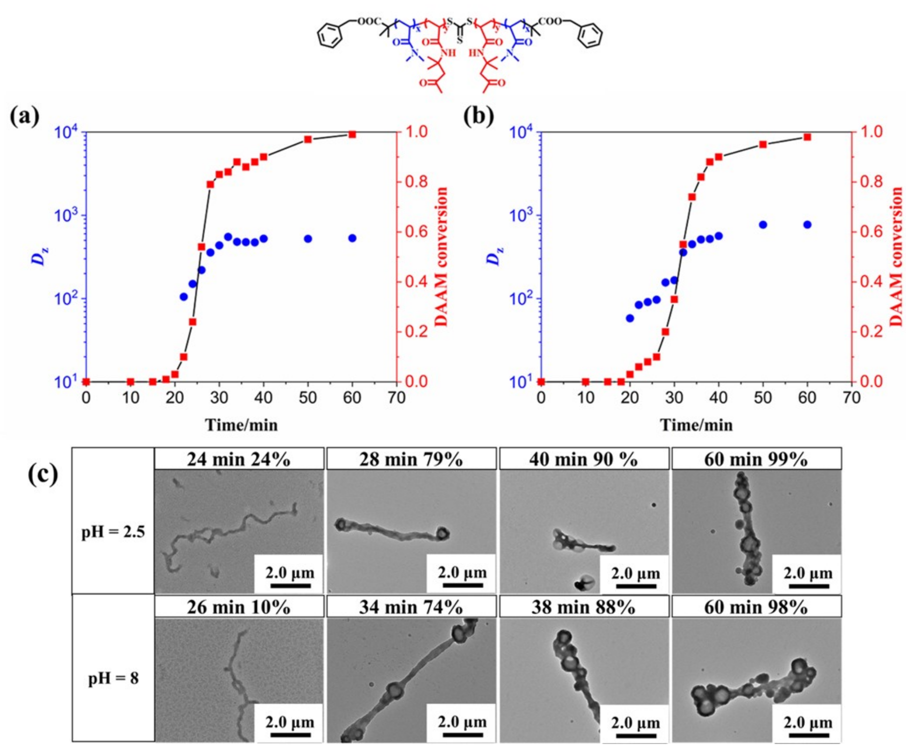

Figure S9. Plots of D_z (blue dots) and DAAM monomer conversion(red squares) as the function of time for benzyl-capped $A_{28}B_{400}A_{28}$ PISA particles prepared at the polymerization pH = (a) 2.5 and (b) 8; (c) TEM images of $A_{28}B_{400}A_{28}$ PISA particles at different reaction time/kinetic conversions under different polymerization pH are presented in.

9. Other Influences on the Morphology of $A_{28}B_yA_{28}$ Copolymers

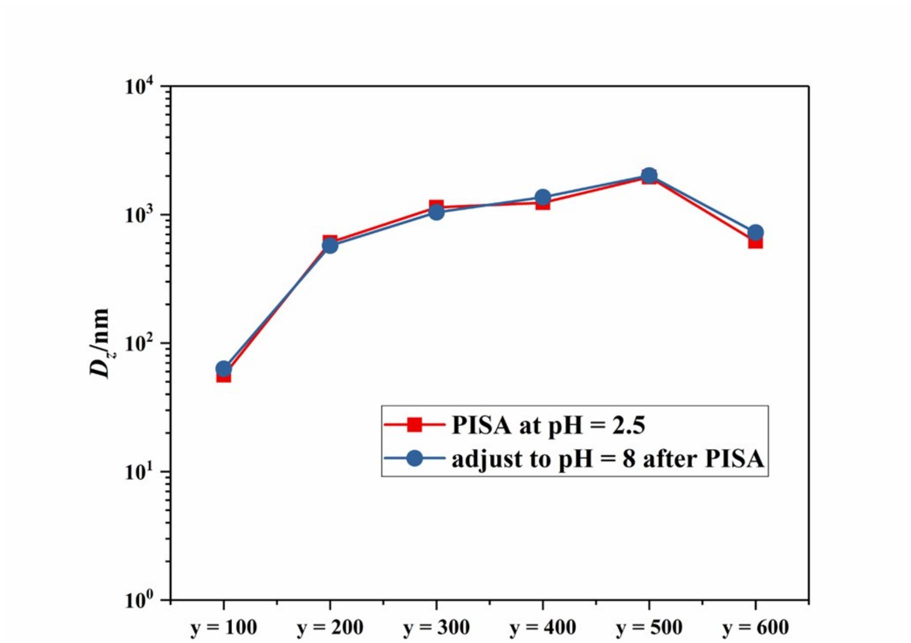

Figure S10. D_z of PISA particles of $A_{28}B_yA_{28}$ as-prepared at the polymerization pH = 2.5 and that post-related at pH = 8 after PISA.

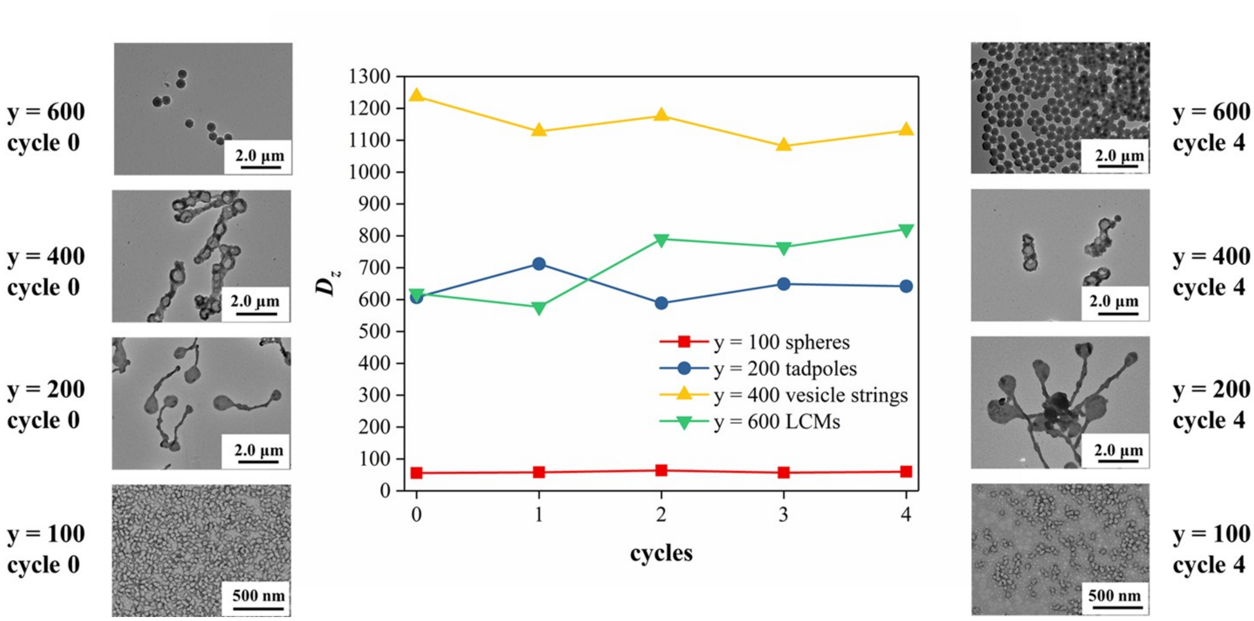

Figure S11. D_z and TEM morphology of $A_{28}B_yA_{28}$ PISA particles prepared at the polymerization pH = 2.5 for four freeze-thaw cycles.

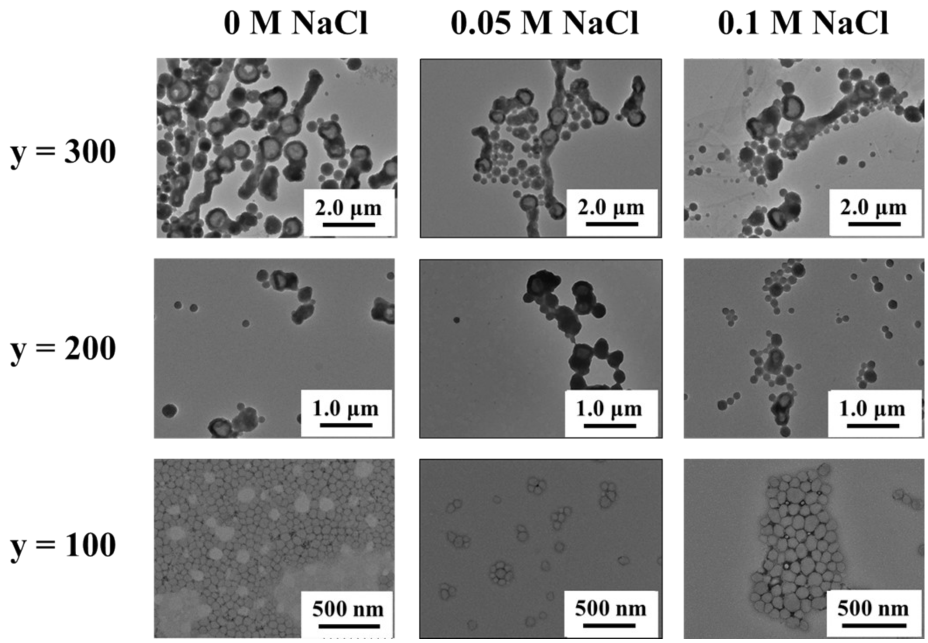

Figure S12. TEM images for $A_{28}B_yA_{28}$ PISA particles polymerized under different NaCl concentrations.

10. The IRI Activity of $A_{28}B_yA_{28}$ Triblock Copolymers

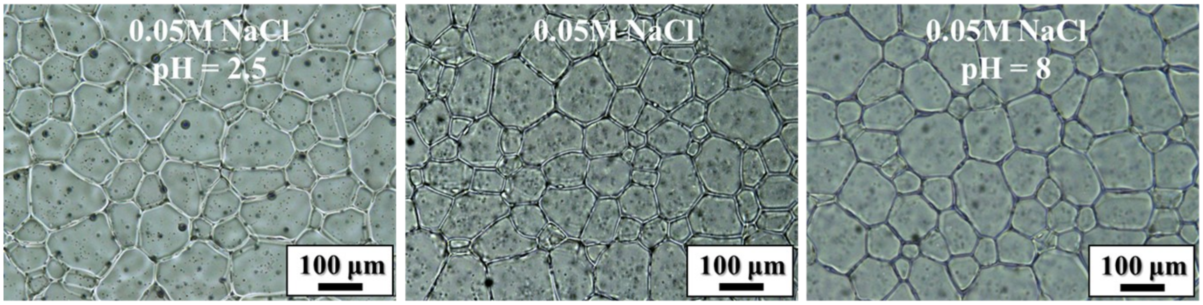

Figure S13. Optical microscope images of recrystallized ice crystals of 0.05 M NaCl at different pHs.

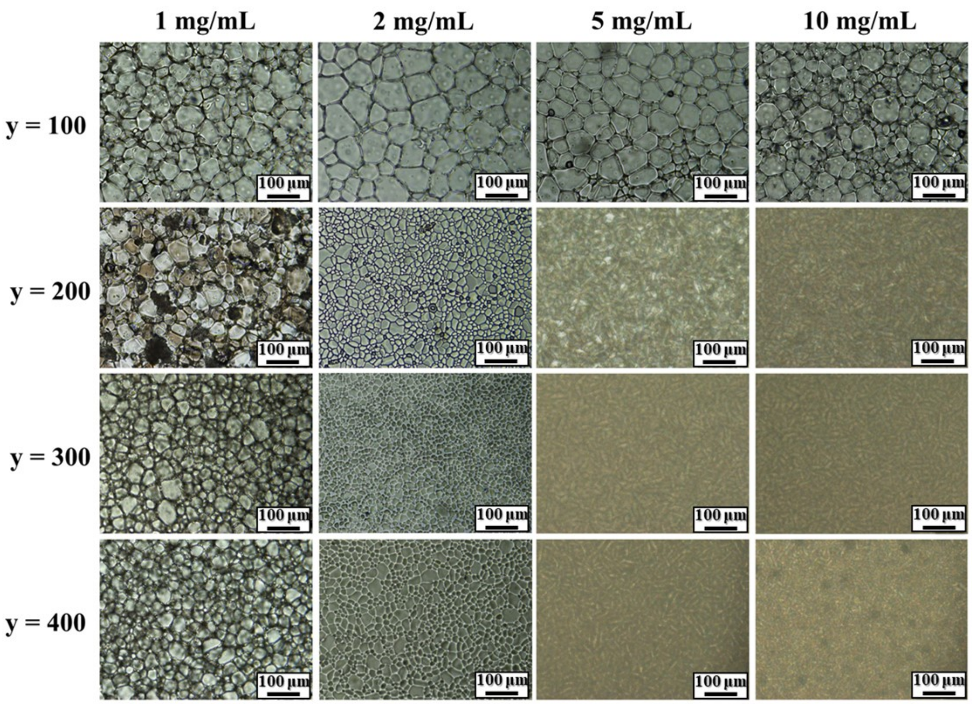

Figure S14. Optical microscope images of recrystallized ice crystals with the participation of $A_{28}B_yA_{28}$ PISA particles with different normalized concentrations of [PDMAA].

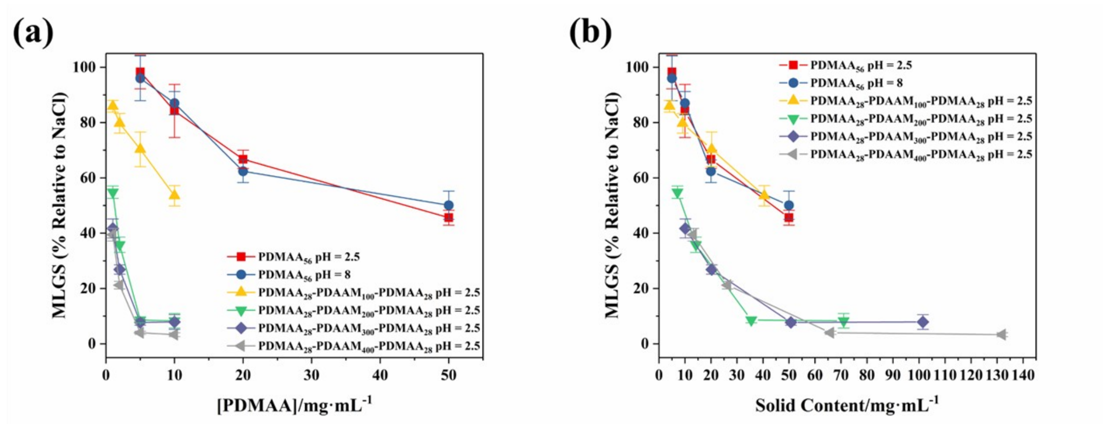

Figure S15. MLGS of $A_{28}B_{y}A_{28}$ PISA particles as the function of (a) [PDMAA] and (b)solid content.

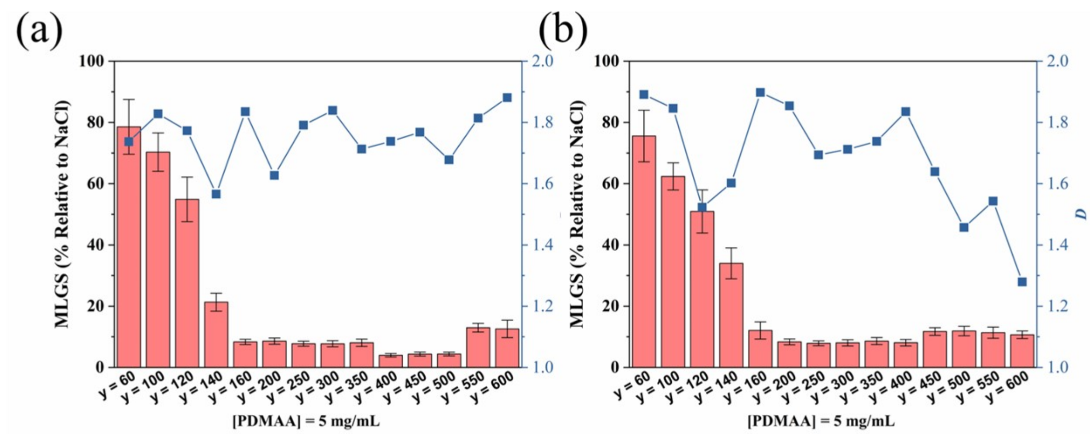

Figure S16. MLGS and fractal dimension (D) as the function of y for $A_{28}B_{y}A_{28}$ PISA particles prepared at the polymerization pH = (a) 2.5 and (b) 6.

11. The DIS Results of $A_{28}B_yA_{28}$ Triblock Copolymers

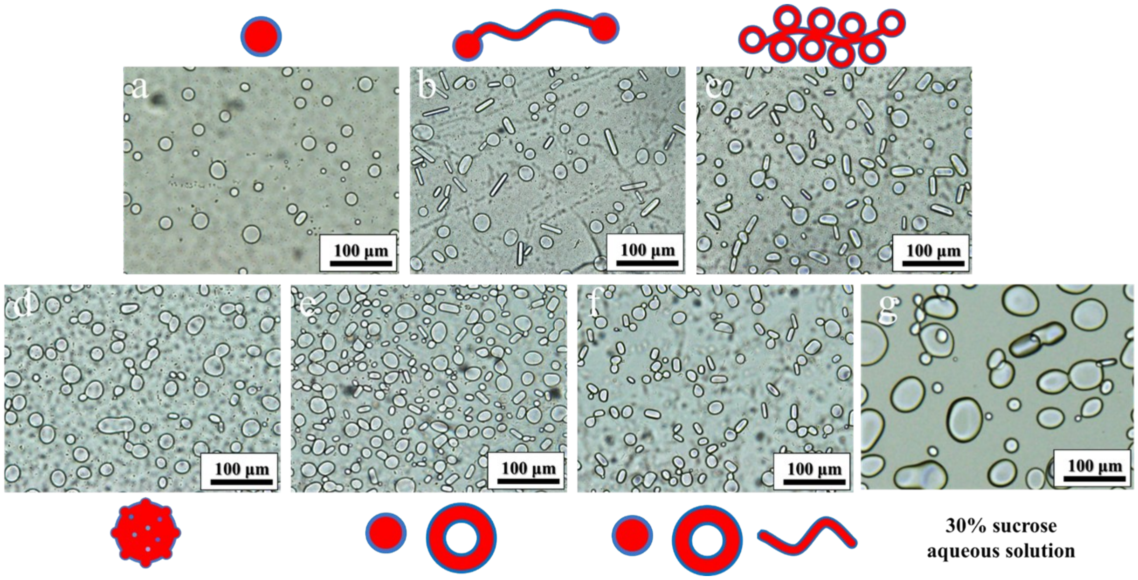

Figure S17. Sucrose-assisted dynamic ice shaping for (a) $A_{28}B_{100}A_{28}$ (pH = 2, spheres, D_z = 56 nm) (b) $A_{28}B_{300}A_{28}$ (pH = 2, tadpoles, D_z = 1139 nm) (c) $A_{28}B_{400}A_{28}$ (pH = 2, vesicle strings, D_z = 1237 nm) (d) $A_{28}B_{600}A_{28}$ (pH = 2, LCVs, D_z = 619 nm) (e) $A_{28}B_{200}A_{28}$ (pH = 6, spheres + vesicles, D_z = 299 nm) (f) $A_{28}B_{300}A_{28}$ (pH = 6, spheres + vesicles + worms, D_z = 570 nm) (g) 30% sucrose aqueous solution The scale bar is 100 µm.

12. The Single Ice Crystal Growth Assay of $A_{28}B_yA_{28}$ Triblock Copolymers

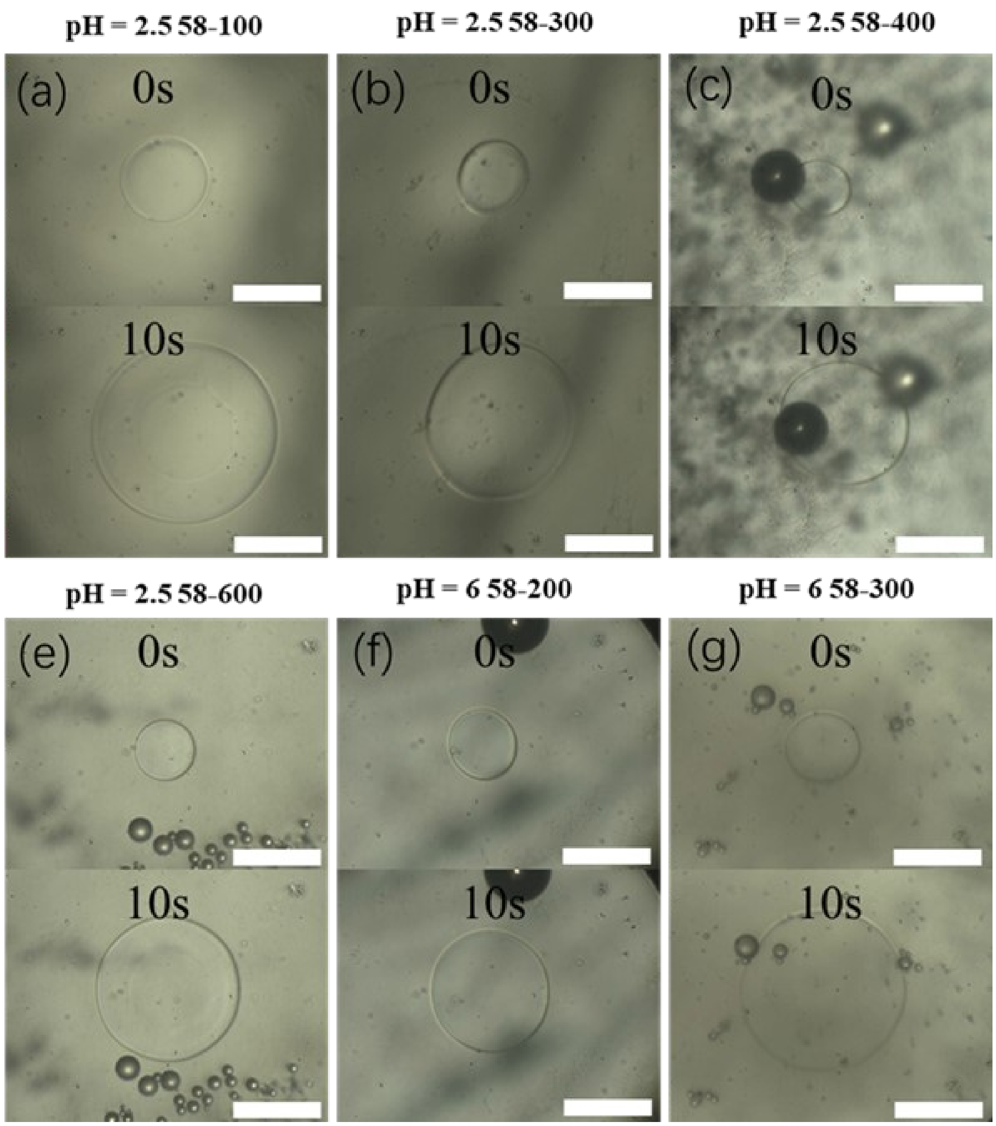

Figure S18. Growth processes of single ice crystals in 1 mg/mL dispersion of (a) $A_{28}B_{100}A_{28}$ (pH = 2, spheres, D_z = 56 nm), (b) $A_{28}B_{300}A_{28}$ (pH = 2, tadpoles, D_z = 1139 nm), (c) $A_{28}B_{400}A_{28}$ (pH = 2, vesicle strings, D_z = 1237 nm), (d) $A_{28}B_{600}A_{28}$ (pH = 2, LCVs, D_z = 619 nm), (e) $A_{28}B_{200}A_{28}$ (pH = 6, spheres + vesicles, D_z = 299 nm) and (f) $A_{28}B_{300}A_{28}$ (pH = 6, spheres + vesicles + worms, D_z = 570 nm). The scale bar is 50 μm.

13. Reference

1. M. Chen, S. Deng, Y. Gu, J. Lin, M. J. MacLeod and J. A. Johnson, *J Am Chem Soc*, 2017, **139**, 2257-2266.
2. J. N. Israelachvili, *Intermolecular and surface forces*, ACADEMIC PR, 1992.